PAPER • OPEN ACCESS

Photoinduced transient states of antiferromagnetic orderings in La$_{1/3}$Sr$_{2/3}$FeO$_3$ and SrFeO$_{3-\delta}$ thin films observed through time-resolved resonant soft x-ray scattering

To cite this article: Kohei Yamamoto *et al* 2022 *New J. Phys.* **24** 043012

View the article online for updates and enhancements.

PAPER

Photoinduced transient states of antiferromagnetic orderings in $La_{1/3}Sr_{2/3}FeO_3$ and $SrFeO_{3-\delta}$ thin films observed through time-resolved resonant soft x-ray scattering

Kohei Yamamoto[1,2,3,*], Tomoyuki Tsuyama[1,4], Suguru Ito[1,2], Kou Takubo[1,5], Iwao Matsuda[1,2], Niko Pontius[6], Christian Schüßler-Langeheine[6], Makoto Minohara[7,8], Hiroshi Kumigashira[7,9], Yuichi Yamasaki[7,10,11,12], Hironori Nakao[7], Youichi Murakami[7], Takayoshi Katase[13], Toshio Kamiya[13] and Hiroki Wadati[1,2,4,14,15]

1 Institute for Solid State Physics, University of Tokyo, Kashiwanoha, Chiba 277-8581, Japan
2 Department of Physics, University of Tokyo, Hongo, Tokyo 113-0033, Japan
3 Institute for Molecular Science, Okazaki, Aichi 444-8585, Japan
4 Department of Applied Physics and Quantum-Phase Electronics Center (QPEC), University of Tokyo, Hongo, Tokyo 113-8656, Japan
5 Department of Chemistry, Tokyo Institute of Technology, Ookayama, Tokyo 152-8551, Japan
6 Helmholtz Zentrum-Berlin für Materialien und Energie GmbH, Albert-Einstein-Straße 15, 12489 Berlin, Germany
7 Photon Factory, Institute of Materials Structure Science, High Energy Accelerator Research Organization (KEK), 1-1 Oho, Tsukuba 305-0801, Japan
8 Research Institute for Advanced Electronics and Photonics, National Institute of Advanced Industrial Science and Technology (AIST), Tsukuba, Ibaraki 305-8568, Japan
9 Institute of Multidisciplinary Research for Advanced Materials (IMRAM), Tohoku University, Sendai 980-8577, Japan
10 National Institute for Materials Science (NIMS), Tsukuba 305-0047, Japan
11 PRESTO, Japan Science and Technology Agency (JST), Saitama 332-0012, Japan
12 RIKEN Center for Emergent Matter Science (CEMS), Wako 351-0198, Japan
13 Laboratory for Materials and Structures, Tokyo Institute of Technology, 4259 Nagatsuta-cho, Midori-ku, Yokohama 226-8503, Japan
14 Department of Material Science, Graduate School of Science, University of Hyogo, Ako, Hyogo 678-1297, Japan
15 Institute of Laser Engineering, Osaka University, Suita, Osaka 565-0871, Japan
* Author to whom any correspondence should be addressed.

E-mail: yamako@ims.ac.jp

Abstract

The relationship between the magnetic interaction and photoinduced dynamics in antiferromagnetic perovskites is investigated in this study. In $La_{1/3}Sr_{2/3}FeO_3$ thin films, commensurate spin ordering is accompanied by charge disproportionation, whereas $SrFeO_{3-\delta}$ thin films show incommensurate helical antiferromagnetic spin ordering due to increased ferromagnetic coupling compared to $La_{1/3}Sr_{2/3}FeO_3$. To understand the photoinduced spin dynamics in these materials, we investigate the spin ordering through time-resolved resonant soft x-ray scattering. In $La_{1/3}Sr_{2/3}FeO_3$, ultrafast quenching of the magnetic ordering within 130 fs through a nonthermal process is observed, triggered by charge transfer between the Fe atoms. We compare this to the photoinduced dynamics of the helical magnetic ordering of $SrFeO_{3-\delta}$. We find that the change in the magnetic coupling through optically induced charge transfer can offer an even more efficient channel for spin-order manipulation.

1. Introduction

In the last century, the challenges in material science have mainly included the observation and manipulation of charges in materials, for application in semiconductor electronics. In the past decades, the utilization of spins, i.e., spintronics, has attracted considerable interest. The faster and energy-efficient

Figure 1. Schematic of the spin and charge ordering in (a) $La_{1/3}Sr_{2/3}FeO_3$ and (b) $SrFeO_{3-\delta}$ (only Fe ions along the 111 direction are depicted).
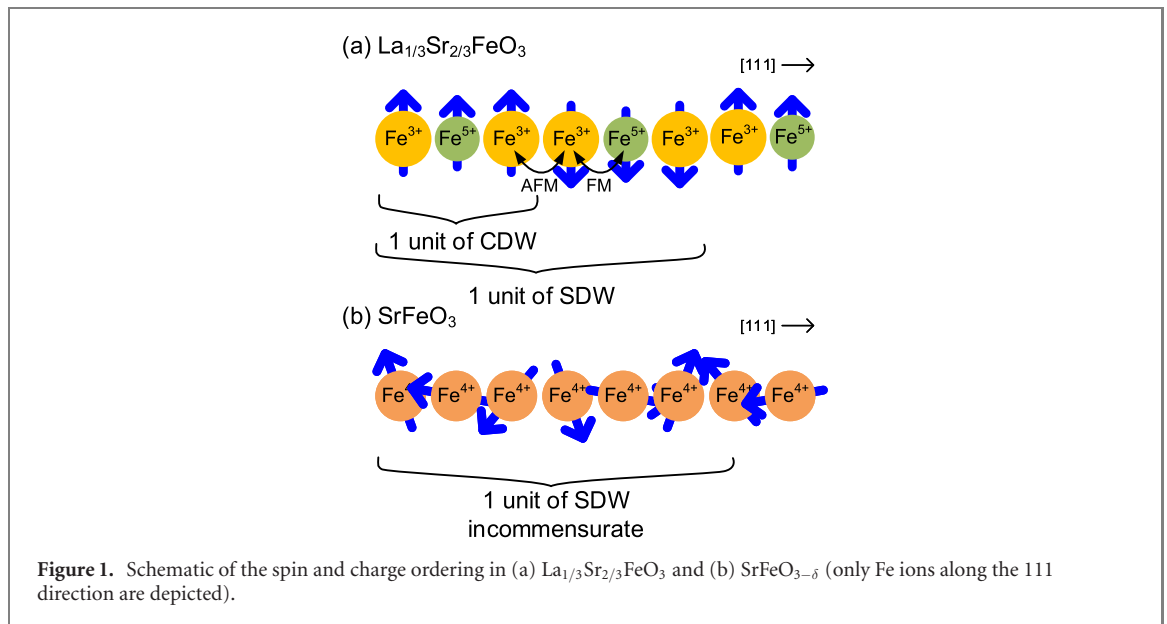
manipulation of spins is one of the main issues in spintronics. Optical control of spins with ultrashort laser pulses is an important research topic for the ultrafast control of magnetization [1]. The first reported ultrafast control involved photoinduced demagnetization in ferromagnetic Ni within 1 ps [2]. Subsequently, the photoinduced charge and spin dynamics have been studied extensively through diffraction and spectroscopy in ferro-, antiferro-, and ferrimagnetic materials [3–13].

Antiferromagnets are expected to be the key material for the photocontrol of magnetic orderings. In the case of ferromagnetic materials, the magnetic moments need to be transferred from the spin to the other degrees-of-freedom, such as the lattice, when the magnetic moments are changed. However, due to the quenched total magnetic moments of antiferromagnets, angular momentum transfer between the spin and other systems is not necessary in antiferromagnets, enabling ultrafast magnetization changes. This was clarified by comparing the ferro- and antiferromagnetic phases of Dy [14].

Several perovskite oxides with antiferromagnetic orderings have been discovered, whose properties can be controlled through elemental substitution and doping because of the strong interactions between the electrons, lattice, and spin degree-of-freedom [15]. Taking advantage of this feature, perovskite oxide materials suitable for the fast optical control of magnetism have been discovered [9, 10, 16, 17]. $La_{1/3}Sr_{2/3}FeO_3$ and $SrFeO_{3-\delta}$ perovskite thin films contain high valence Fe ions and oxygen holes. These features are clearly different from ordinary metals and insulators. In particular, $La_{1/3}Sr_{2/3}FeO_3$ has charge and spin ordered structure with three and six Fe ions period and ordered structures such as this are realized in a few perovskites. We focused on antiferromagnetic orderings of Fe perovskite oxides and surveyed the photoinduced dynamics of these orderings directly.

The equilibrium magnetic properties of $La_{1-x}Sr_xFeO_3$ perovskites can be controlled based on the La/Sr composition. $La_{1/3}Sr_{2/3}FeO_3$ thin films exhibit a charge disproportionation (CD) of $3Fe^{3.67+} \rightarrow Fe^{5+} + 2Fe^{3+}$ accompanying antiferromagnetic ordering below $T_N = T_{CD} \approx 190$ K [18, 19]. The high valence state of Fe^{5+} is realized as $Fe^{3+}\underline{L}^2$, where $\underline{L}$ denotes an oxygen $2p$ hole [20]. This CD phase results in a charge density wave with a period comprising three Fe ions as that of the crystal lattice, and a spin density wave of six Fe ion period along the 111 directions, as revealed by a neutron diffraction study (see figure 1(a)) [15]. $SrFeO_{3-\delta}$ includes the Fe^{4+} ion and shows a helimagnetic phase with incommensurate periodicity, which occurs because of the competition between the nearest neighbor ferromagnetic and the next-nearest neighbor antiferromagnetic interaction of the conducting $3d$ electrons, as indicated by neutron scattering results [21]. Fe^{4+} is realized as the $Fe^{3+}\underline{L}$ in $SrFeO_3$ perovskites [20, 22]. T_N was reported to be 134 K [21] (bulk), ≈ 105 K [23], ≈ 115 K [24] (thin films). A multiple Q helimagnetic phase in $SrFeO_{3-\delta}$ was argued [23, 25], which could possibly host skyrmion crystals [26].

Resonant soft x-ray scattering (RSXS) [27] is a powerful tool for revealing the ordered structures in solids, such as the magnetic, charge, and orbital ordering [27–33]. RSXS can be performed with the core level absorption process, and the interaction between x-rays and a specific element can be enhanced. Hence, RSXS can be applied to thin films with small sample volumes. X-ray polarization is sensitive to the orbitals of the valence electrons and RSXS can detect orbital and spin ordering, which are coupled through spin-orbit interaction. The magnetic ordering of irons in $La_{1/3}Sr_{2/3}FeO_3$ [33, 34] and $SrFeO_{3-\delta}$ [23] have been observed through RSXS at the Fe $L_{2,3}$ absorption edge ($2p \rightarrow 3d$, ≈ 709 eV).

In this study, we report the photoinduced magnetic dynamics of $La_{1/3}Sr_{2/3}FeO_3$ and $SrFeO_{3-\delta}$ thin films determined through time-resolved RSXS measurements. We ascertain the ultrafast melting of the $La_{1/3}Sr_{2/3}FeO_3$ magnetic ordering through charge transfer between Fe ions, which can be attributed to the strong coupling between the charge and spin in the system. Based on the comparison between $La_{1/3}Sr_{2/3}FeO_3$ and $SrFeO_{3-\delta}$, the effect of the electronic properties on the dynamics of the photoinduced quenching of the magnetic orderings is examined.
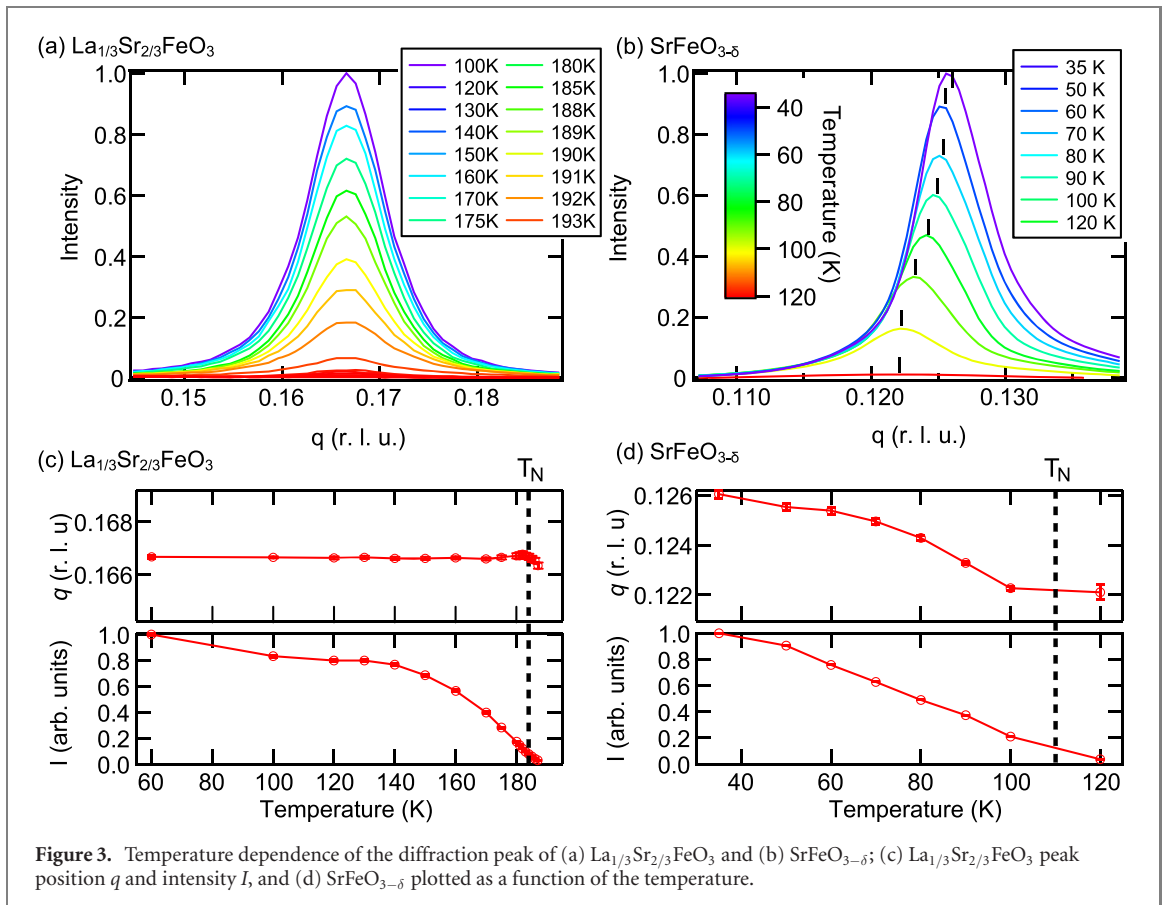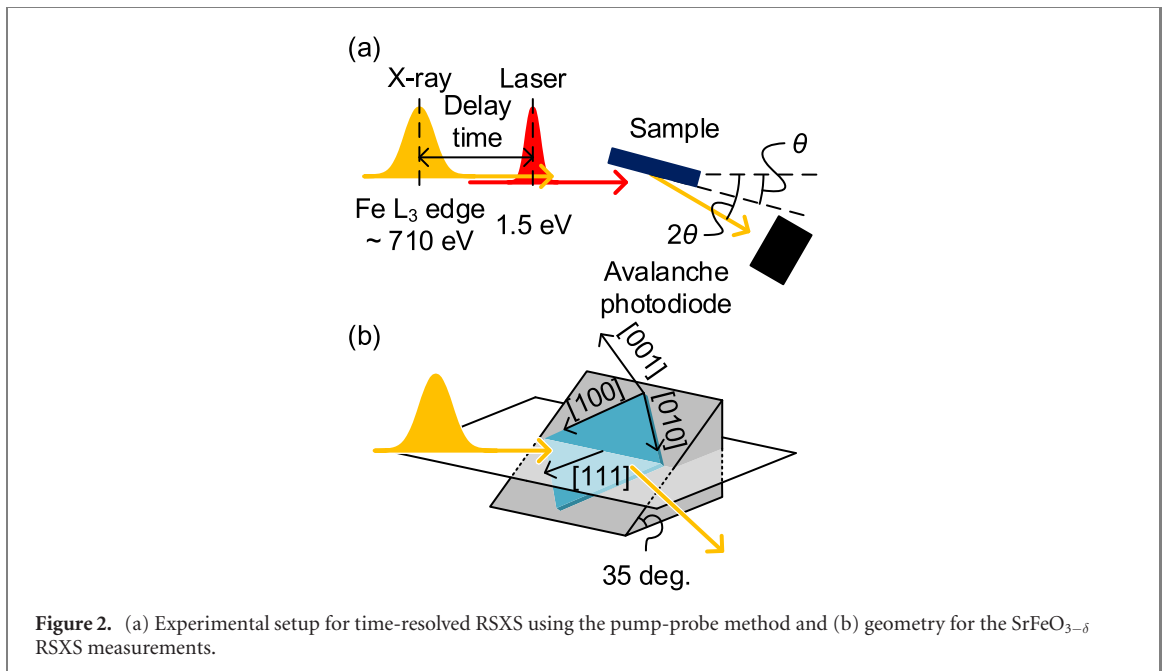
2. Experimental

$La_{1/3}Sr_{2/3}FeO_3$ thin films with ≈ 40 nm thicknesses were grown epitaxially on $SrTiO_3$ (111) substrates using the pulsed laser deposition method. The details of the synthesis of $La_{1/3}Sr_{2/3}FeO_3$ can be found in reference [35]. The magnetic ordering along [111] direction of $La_{1/3}Sr_{2/3}FeO_3$ was more stabilized than the other $\langle 111 \rangle$ direction owing to the rhombohedral distortion [34]. By oxidizing $SrFeO_{2.5}$ grown epitaxially on $SrTiO_3$ (100) substrates using the pulsed laser deposition method, $SrFeO_{3-\delta}$ thin films with ≈ 27 nm thicknesses were fabricated on $SrTiO_3(100)$. $SrFeO_{3-\delta}$ was obtained by annealing $SrFeO_{2.5}$ in an ozone atmosphere at 300 °C for 6 h with the sample exposed to UV light in a UV/O3 DRY CLEANER UV-1 (SAMCO Inc.). While, $SrFeO_3$ is metallic, $SrFeO_{3-\delta}$ is semiconductive and this introduced δ of our samples enables the comparison to the insulating $La_{1/3}Sr_{2/3}FeO_3$. In $SrFeO_{3-\delta}$ thin films, all $\langle 111 \rangle$ directions are equivalent and we observed one of four equivalent $\langle 111 \rangle$ directions.

In order to elucidate the photoinduced dynamics of the antiferromagnetic ordering in $La_{1/3}Sr_{2/3}FeO_3$ and $SrFeO_{3-\delta}$, we performed time-resolved RSXS measurements using the pump-probe method at the slicing facility UE56/1-ZPM Helmholtz-Zentrum, Berlin [36]. The experimental setup is shown in figure 2. A Ti:sapphire laser ($\lambda = 800$ nm, 1.5 eV) was employed for photoexcitation, with a pulse duration of 50 fs. The spot size of the pump laser was $\sim 600 \, \mu m \times \sim 400 \, \mu m$, and that of the probe x-ray was $\sim 150 \, \mu m \times \sim 30 \, \mu m$ [36]. The separation angle of both beams was smaller than 2° and this separation angle had a negligible effect on the delay time error within the overall temporal resolution of the experiment. The laser and x-ray pulse frequencies were 3 and 6 kHz, respectively, and signals with and without pump laser excitation were obtained alternately. The signals without excitation were used for normalizing the pumped signals. The scattered x-rays were detected using an avalanche photodiode. The laser slicing facility at BESSY has two operation modes: one with 50 ps temporal resolution and high pulse energy and one with 130 fs temporal resolution and low pulse energy. We used 50 ps x-ray pulses to obtain the outline of the photo-induced dynamics of $La_{1/3}Sr_{2/3}FeO_3$ and $SrFeO_{3-\delta}$ and then investigated the detailed dynamics of $La_{1/3}Sr_{2/3}FeO_3$ using 100 fs x-ray pulses generated using the laser slicing technique [36]. The total time resolution was ≈ 130 fs. The scattering intensity from $SrFeO_{3-\delta}$ was too small for experiments with the weak 100 fs x-ray pulses. So we restricted ourselves to the lower temporal resolution of about 50 ps. $SrFeO_{3-\delta}$ was mounted on a wedge-shaped jig at an angle of 55 deg. in order to orient the [111] direction in the scattering plane, and the temperature was set to 35 K. We set the x-ray photon energy and polarization to the Fe L_3 edge (≈ 710 eV) and horizontal, respectively, for obtaining the magnetic signals. Static $La_{1/3}Sr_{2/3}FeO_3$ measurements were performed with a diffractometer at the soft x-ray beamline BL-16A, Photon Factory, KEK, Japan [37]. The experimental geometry and temperature were equivalent to the time-resolved measurement, and a silicon drift detector was used.

3. Results and discussion

Figure 3 depicts the $Q = (q, q, q)$ antiferromagnetic ordering peaks of (a) $La_{1/3}Sr_{2/3}FeO_3$ and (b) $SrFeO_{3-\delta}$. The diffraction peaks were scanned along the [111] direction. The temperature dependence of q and the peak intensities of $La_{1/3}Sr_{2/3}FeO_3$ and $SrFeO_{3-\delta}$ are displayed in figures 3(c) and (d) respectively. The temperature evolution of RSXS intensity reproduced results of the previous study Néel temperature T_N was determined via power-law fit ($\propto |T - T_N|^{\nu}$) of peak intensity, as shown in figures 3(c) and (d). T_N of $La_{1/3}Sr_{2/3}FeO_3$ and $SrFeO_{3-\delta}$ was estimated to be 187 K and 110 K, respectively. For the $La_{1/3}Sr_{2/3}FeO_3$ thin films, the peak position is fixed at $(1/6, 1/6, 1/6)$ in the entire temperature range below T_N, as shown in figure 3(a). The $SrFeO_{3-\delta}$ diffraction peak appears below $T_N \approx 110$ K, and the peak position shifts according to the temperature. Our $SrFeO_{3-\delta}$ thin films show the helimagnetic ordering below $T_N = 110$ K with $q = 0.126$ r.l.u. along with insulating feature, which implies that δ of our $SrFeO_{3-\delta}$ samples is ~ 0.15 by comparing it with the results of previous studies [23, 24, 38, 39]. q of the $SrFeO_{3-\delta}$ helimagnetic ordering was reported to be 0.128–0.112 ($SrFeO_{2.87}$) [21, 40], 0.13 ($SrFeO_{3-\delta}$) or 0.125 ($Sr_{0.99}Co_{0.01}FeO_3$) [23]; our observed $q = 0.126$ is in a similar range. In the heating and cooling cycle, thermal hysteresis was observed for the peak intensity and peak positions. The hysteresis has been reported to be related to the

Figure 2. (a) Experimental setup for time-resolved RSXS using the pump-probe method and (b) geometry for the SrFeO$_{3-\delta}$ RSXS measurements.

Figure 3. Temperature dependence of the diffraction peak of (a) La$_{1/3}$Sr$_{2/3}$FeO$_3$ and (b) SrFeO$_{3-\delta}$; (c) La$_{1/3}$Sr$_{2/3}$FeO$_3$ peak position q and intensity I, and (d) SrFeO$_{3-\delta}$ plotted as a function of the temperature.

phase separation of paramagnetic and antiferromagnetic phases [41]. Similar phase separation was pointed out in La$_{1/3}$Sr$_{2/3}$FeO$_3$ [34]. According to previous resistivity measurement reports [23, 24], thermal hysteresis was observed at $T = 46$–71 K, and our observed thermal hysteresis reflects this phenomenon.

We first discuss the La$_{1/3}$Sr$_{2/3}$FeO$_3$ dynamics. The time evolution of the magnetic peak intensity after laser pumping, revealed in the laser slicing mode, is shown in figure 4(a). Rapid reduction in the diffraction intensity is observed within a time resolution of 130 fs. The diffraction intensities decrease to 50% of the initial values with the fluence of 0.5 mJ cm^{-2}. This fluence corresponds to $\approx$0.03 photons/unit cell assuming absorption coefficient of 1.7×10^5 cm^{-1} [17] and unit cell volume of (0.39 nm)^3. We confirmed

Figure 4. (a) Time evolution of the magnetic peak intensity of $La_{1/3}Sr_{2/3}FeO_3$ at $\tau_{resolution} = 130$ fs for various pump laser fluence obtained in the laser slicing mode (the solid lines are fitted to the data using equation (1)) and (b) illustration of the photoinduced transient states of $La_{1/3}Sr_{2/3}FeO_3$.
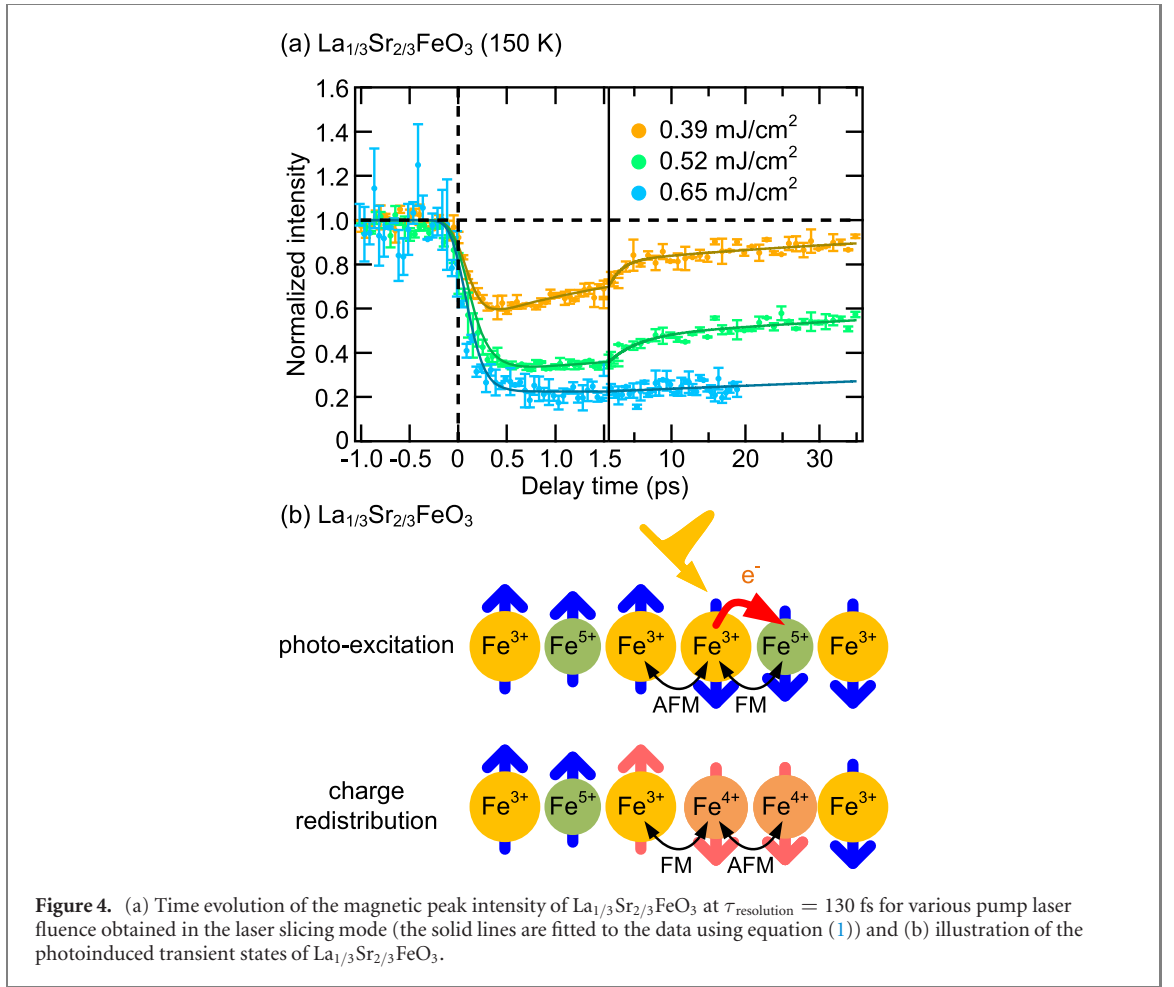
Table 1. Fitting parameters for the delay scans of the $La_{1/3}Sr_{2/3}FeO_3$ RSXS intensities in figure 4(a) observed in the slicing mode. $\tau_{resolution} = 130$ fs. τ_{decay} is less than time resolution $\tau_{resolution}$.

Fluence (mJ cm^{-2})	$R + R_{fast}$	τ_{fast} (ps)	τ (ps)
0.39	0.51 ± 0.05	1.7 ± 0.3	60 ± 11
0.52	0.72 ± 0.03	3.5 ± 1.0	210 ± 36
0.65	0.78 ± 0.08	—	550 ± 100

that the intensity of unpumped signal intensity remained unchanged due to the pump laser fluence, which implies that the base temperature was constant. The decreased diffraction intensity recovers 30 ps after laser excitation in the lower fluence regime; however, the recovery is slower at higher fluence. In order to discuss the results quantitatively, we fitted them using the function depicted by equation (1) for the decay and recovery processes. The fitting function is as follows:

$$f(t) = 1 + \left[(R_{fast} + R) \exp\left(\frac{-t}{\tau}\right) - R_{fast} \exp\left(\frac{-t}{\tau_{fast}}\right) - R \exp\left(\frac{-t}{\tau_{decay}}\right) \right] H(t) * \exp\left(-\frac{\ln(2)}{4} \frac{t^2}{\tau_{resolution}^2}\right),$$

(1)

where τ_{decay} describes the time constant for photo-induced reduction, τ_{fast} and τ describe the time constants for the fast and slower components of recovery with an amplitude of R_{fast} and R. To consider time resolution, the fitting function was convoluted by a Gaussian with a full-width-at-half-maximum of $\tau_{resolution} = 130$ fs. The parameters extracted from the experimental delay scans are summarized in table 1. The τ_{decay} time scale was estimated to be 0.1 ± 0.05 ps.

For the nonthermal $La_{1/3}Sr_{2/3}FeO_3$ process with an ultrashort time scale of $\tau_{decay} \leqslant 0.1$ ps, we consider that the ultrafast magnetization dynamics occurs because of the ultrafast photo-melting of the charge ordering, which destroys the magnetic ordering due to the strong coupling between the charge and spin. Demagnetization due to the photo-melting of the charge ordering has also been observed, for example, in NdNiO$_3$ thin films [9]. Figure 4(b) illustrates the origins of the ultrafast melting of the magnetic ordering.

Table 2. Fitting parameters for the delay scans of the $La_{1/3}Sr_{2/3}FeO_3$ and $SrFeO_{3-\delta}$ RSXS intensities in figure 5 with the $\tau_{resolution} = 130$ fs. τ_{decay} is less than time resolution $\tau_{resolution}$. τ was not suitably determined due to the small temporal scan range.

|	Fluence (mJ cm^{-2})	R	τ (ps)
$La_{1/3}Sr_{2/3}FeO_3$	0.26	0.070 ± 0.002	—
	0.39	0.169 ± 0.003	—
	0.46	0.300 ± 0.004	—
	0.52	0.514 ± 0.004	—
	0.65	0.701 ± 0.003	—
	0.78	0.759 ± 0.004	—
$SrFeO_{3-\delta}$	0.71	0.14 ± 0.02	542 ± 196
	1.41	0.16 ± 0.03	335 ± 76
	2.12	0.44 ± 0.03	308 ± 41
	2.82	0.54 ± 0.03	357 ± 42

Due to the strong onsite Hund's rule coupling, excitation with linearly polarized light at 1.5 eV can result only in transitions between the ferromagnetically coupled sites [42]. Optical conductivity measurement has demonstrated that the optical gap of 0.15 eV has a strong interatomic d–d transition characteristic [42]. Therefore, the excited electron would be transferred only in the ferromagnetically coupled Fe^{3+}–Fe^{5+}–Fe^{3+} sites, and the observation in this study suggests that the excitation induces charge transfer in a unit of the charge-ordering site of Fe^{3+}–Fe^{5+}–Fe^{3+} into Fe^{3+}–Fe^{4+}–Fe^{4+}, as shown in figure 4(b). It has been suggested that this charge transfer is a metastable state accompanying Fe–O bond-length change, in a previous report on the photoinduced transient states of $La_{1/3}Sr_{2/3}FeO_3$ [43]. Transfer in the charge ordering induces changes in the magnetic interactions. Fe^{3+}–Fe^{4+} ions have ferromagnetic interactions, whereas the Fe^{4+}–Fe^{4+} sites have antiferromagnetic ones, as shown in figure 4(b).

Furthermore, time-resolved RSXS measurements were performed for 35 and 80 K $SrFeO_{3-\delta}$ thin films as shown in figure 5(a) with a time resolution of $\tau_{resolution} \approx 50$ ps; the experimental results for $La_{1/3}Sr_{2/3}FeO_3$ with a similar time resolution are also shown in the right panel for comparison. Due to $\tau_{resolution} \approx 50$ ps, the fast decay process cannot be resolved in figure 5(a), and we focus on the changes in the magnetic ordering peak intensity. We fitted the results using equation (1) with setting the values of R_{fast}, τ_{decay}, and τ_{fast} to 0 because fast component cannot be observed due to the lower time resolution. The function for fitting is

$$f(t) = \left[1 - R \exp\left(\frac{-t}{\tau} \right) H(t) \right] * \exp\left(-\frac{\ln(2)}{4} \frac{t^2}{\tau_{resolution}^2} \right). \tag{2}$$

The degrees of quenching R, defined by equation (2), of the $La_{1/3}Sr_{2/3}FeO_3$ and $SrFeO_{3-\delta}$ magnetic ordering are plotted as a function of the laser fluence in figure 5(b). For $La_{1/3}Sr_{2/3}FeO_3$, the quenching of the peak intensity reaches $\approx 70\%$ at a fluence of approximately 0.75 mJ cm^{-2}; however, the $SrFeO_{3-\delta}$ diffraction intensity decreases by less than 60% of the initial intensity below a fluence of 2.8 mJ cm^{-2}. This suggests that the antiferromagnetic ordering of $La_{1/3}Sr_{2/3}FeO_3$ is quenched with less excitation energy compared to $SrFeO_{3-\delta}$. It should be noted that we observed ultrafast reduction of peak intensity of $La_{1/3}Sr_{2/3}FeO_3$ with the time resolution of 130 fs and we compared $La_{1/3}Sr_{2/3}FeO_3$ and $SrFeO_{3-\delta}$ results based on the experiments of which time resolution is 50 ps. The electron temperature increase is estimated to be about several hundred K, which is in the similar range of previous studies [2, 5]. The peak positions of the photoinduced transient states and the heating process are plotted as a function of the peak area intensity in figure 5(c). The diffraction peaks of the transient states are shown in figure 5(d). Area intensities are obtained as the integration of the diffraction peak scan. Both curves are similar, indicating that the observed photoinduced quenching of the $SrFeO_{3-\delta}$ helimagnetic ordering is triggered by the same mechanism as the temperature-induced change (table 2).

$SrFeO_3$ is metallic and 1.5 eV laser excitation corresponds to the interband transition [44]. The photoinduced quenching of the helimagnetic ordering in $SrFeO_{3-\delta}$ can be interpreted as the result of the increase in the spin and electron temperatures, as depicted in figure 5(e). On the other hand, $La_{1/3}Sr_{2/3}FeO_3$ is insulating and its magnetic orderings disappear because of the charge transfer between Fe ions induced locally by photoexcitation, as discussed above. The photoinduced dynamics of the antiferromagnetic orderings reflect the versatile electronic feature of perovskite oxides. Owing to the Sr substitution dependence of the absorption coefficient [17], the absorption coefficient becomes larger, which indicates that the observed trend does not originate from the strong absorption.
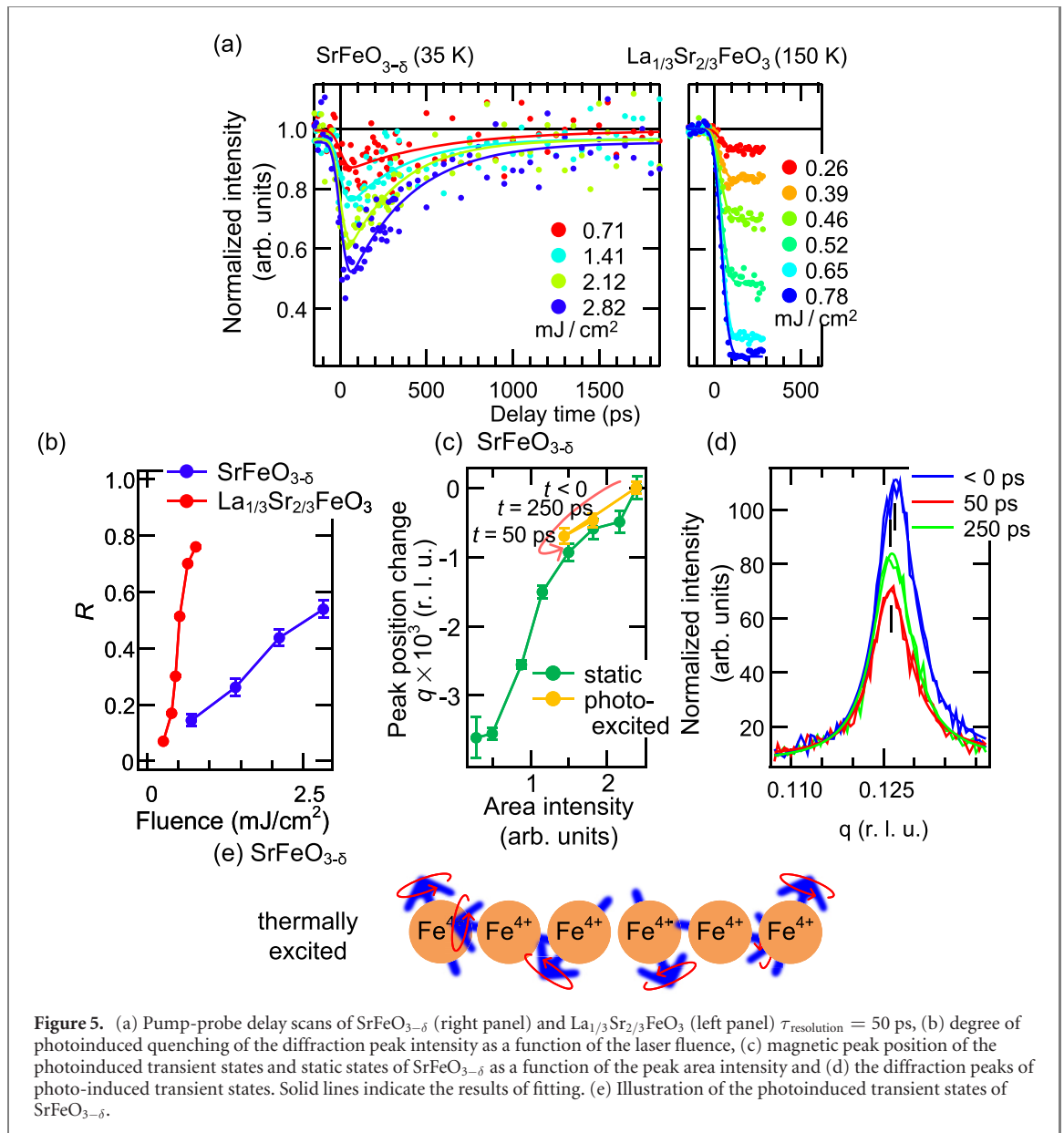
Figure 5. (a) Pump-probe delay scans of SrFeO$_{3-\delta}$ (right panel) and La$_{1/3}$Sr$_{2/3}$FeO$_3$ (left panel) $\tau_{\text{resolution}} = 50$ ps, (b) degree of photoinduced quenching of the diffraction peak intensity as a function of the laser fluence, (c) magnetic peak position of the photoinduced transient states and static states of SrFeO$_{3-\delta}$ as a function of the peak area intensity and (d) the diffraction peaks of photo-induced transient states. Solid lines indicate the results of fitting. (e) Illustration of the photoinduced transient states of SrFeO$_{3-\delta}$.

4. Conclusion

In this study, we examined the photoinduced dynamics of the antiferromagnetic orderings in two perovskites, La$_{1/3}$Sr$_{2/3}$FeO$_3$ and SrFeO$_{3-\delta}$, through time-resolved RSXS. The magnetic ordering in La$_{1/3}$Sr$_{2/3}$FeO$_3$ thin films was quenched within 130 fs. This ultrafast dynamics can be explained based on the photoinduced charge transfer between Fe ions, which induces a change in the strong magnetic interactions. The process is nonthermal. The spin moment can be canceled with the nearest neighbors in antiferromagnetic La$_{1/3}$Sr$_{2/3}$FeO$_3$ through this ultrafast process, leading to an ultrafast photoinduced change in the magnetic ordering. Compared to helimagnetic SrFeO$_{3-\delta}$, the magnetic ordering of La$_{1/3}$Sr$_{2/3}$FeO$_3$ was destroyed at lower fluence. Spin manipulation in helical systems has been found to be more energy efficient than in ferromagnets. An even more energy-efficient process can be realized in La$_{1/3}$Sr$_{2/3}$FeO$_3$. Ultrafast changes in the magnetic ordering of antiferromagnetic perovskite thin films were discovered, and the photoinduced dynamics was shown to be controlled by tuning the electronic feature through perovskite doping. However, this comparison does leave aside the possibility that a strong reduction of the SrFeO$_{3-\delta}$ antiferromagnetic peak intensity was neglected due to the lower time resolution compared to La$_{1/3}$Sr$_{2/3}$FeO$_3$ case. Further investigations with better time resolution are needed in order to determine the time evolution of antiferromagnetic orderings completely. Changes of substrates or thickness affect the nature of thin films and such parameters characteristic of thin films are important to control the photo-induced magnetization dynamics. The photoinduced dynamics of the spin order in antiferromagnetic perovskite thin films is important for integrating functional oxides into spintronic device architectures.

Acknowledgments

Data availability statement

The data that support the findings of this study are available upon reasonable request from the authors.

ORCID iDs

Kohei Yamamoto ⓘ https://orcid.org/0000-0002-4270-6410
Kou Takubo ⓘ https://orcid.org/0000-0002-2591-1244
Iwao Matsuda ⓘ https://orcid.org/0000-0002-2118-9303
Niko Pontius ⓘ https://orcid.org/0000-0002-5658-1751
Christian Schüßler-Langeheine ⓘ https://orcid.org/0000-0002-4553-9726
Makoto Minohara ⓘ https://orcid.org/0000-0003-4367-9175
Hiroshi Kumigashira ⓘ https://orcid.org/0000-0003-4668-2695
Hironori Nakao ⓘ https://orcid.org/0000-0003-4020-537X
Takayoshi Katase ⓘ https://orcid.org/0000-0002-2593-7487
Hiroki Wadati ⓘ https://orcid.org/0000-0001-5969-8624

References

[1] Kirilyuk A, Kimel A V and Rasing T 2010 *Rev. Mod. Phys.* **82** 2731–84
[2] Beaurepaire E, Merle J-C, Daunois A and Bigot J-Y 1996 *Phys. Rev. Lett.* **76** 4250–3
[3] Stamm C *et al* 2007 *Nat. Mater.* **6** 740–3
[4] Stanciu C D, Hansteen F, Kimel A V, Kirilyuk A, Tsukamoto A, Itoh A and Rasing T 2007 *Phys. Rev. Lett.* **99** 047601
[5] Koopmans B, Malinowski G, Longa F D, Steiauf D, Fähnle M, Roth T, Cinchetti M and Aeschlimann M 2010 *Nat. Mater.* **9** 259–65
[6] Radu I *et al* 2011 *Nature* **472** 205–8
[7] Johnson S L *et al* 2012 *Phys. Rev. Lett.* **108** 037203
[8] Lee W S *et al* 2012 *Nat. Commun.* **3** 838
[9] Caviglia A D *et al* 2013 *Phys. Rev.* B **88** 220401
[10] Beaud P *et al* 2014 *Nat. Mater.* **13** 923–7
[11] Först M *et al* 2014 *Phys. Rev. Lett.* **112** 157002
[12] Först M *et al* 2015 *Nat. Mater.* **14** 883–8
[13] Tsuyama T, Chakraverty S, Macke S, Pontius N, Schüßler-Langeheine C, Hwang H Y, Tokura Y and Wadati H 2016 *Phys. Rev. Lett.* **116** 256402
[14] Thielemann-Kühn N, Schick D, Pontius N, Trabant C, Mitzner R, Holldack K, Zabel H, Föhlisch A and Schüßler-Langeheine C 2017 *Phys. Rev. Lett.* **119** 197202
[15] Imada M, Fujimori A and Tokura Y 1998 *Rev. Mod. Phys.* **70** 1039–263
[16] Miyasaka K, Nakamura M, Ogimoto Y, Tamaru H and Miyano K 2006 *Phys. Rev.* B **74** 012401
[17] Smolin S Y, Scafetta M D, Choquette A K, Sfeir M Y, Baxter J B and May S J 2016 *Chem. Mater.* **28** 97–105
[18] Wadati H *et al* 2005 *Phys. Rev.* B **71** 035108
[19] Sichel-Tissot R J, Devlin R C, Ryan P J, Kim J-W and May S J 2013 *Appl. Phys. Lett.* **103** 212905
[20] Abbate M *et al* 1992 *Phys. Rev.* B **46** 4511–9
[21] Takeda T, Yamaguchi Y and Watanabe H 1972 *J. Phys. Soc. Japan* **33** 967–9
[22] Bocquet A E, Fujimori A, Mizokawa T, Saitoh T, Namatame H, Suga S, Kimizuka N, Takeda Y and Takano M 1992 *Phys. Rev.* B **45** 1561–70
[23] Chakraverty S *et al* 2013 *Phys. Rev.* B **88** 220405
[24] Rogge P C, Green R J, Sutarto R and May S J 2019 *Phys. Rev. Mater.* **3** 084404
[25] Ishiwata S *et al* 2011 *Phys. Rev.* B **84** 054427
[26] Ishiwata S *et al* 2020 *Phys. Rev.* B **101** 134406
[27] Fink J, Schierle E, Weschke E and Geck J 2013 *Rep. Prog. Phys.* **76** 056502
[28] Schüßler-Langeheine C *et al* 2001 *J. Electron Spectrosc. Relat. Phenom.* **114–116** 953–7
[29] Zhou S Y *et al* 2011 *Phys. Rev. Lett.* **106** 186404
[30] Partzsch S, Wilkins S B, Hill J P, Schierle E, Weschke E, Souptel D, Büchner B and Geck J 2011 *Phys. Rev. Lett.* **107** 057201
[31] Wadati H *et al* 2012 *Phys. Rev. Lett.* **108** 047203
[32] Matsuda T *et al* 2015 *Phys. Rev. Lett.* **114** 236403

[33] Yamamoto K *et al* 2018 *Phys. Rev. B* **97** 075134
[34] Okamoto J *et al* 2010 *Phys. Rev. B* **82** 132402
[35] Minohara M, Kitamura M, Wadati H, Nakao H, Kumai R, Murakami Y and Kumigashira H 2016 *J. Appl. Phys.* **120** 025303
[36] Holldack K *et al* 2014 *J. Synchrotron Radiat.* **21** 1090–104
[37] Nakao H, Yamasaki Y, Okamoto J, Sudayama T, Takahashi Y, Kobayashi K, Kumai R and Murakami Y 2014 *J. Phys.: Conf. Ser.* **502** 012015
[38] Adler P, Lebon A, Damljanović V, Ulrich C, Bernhard C, Boris A V, Maljuk A, Lin C T and Keimer B 2006 *Phys. Rev. B* **73** 094451
[39] MacChesney J B, Sherwood R C and Potter J F 1965 *J. Chem. Phys.* **43** 1907–13
[40] Reehuis M, Ulrich C, Maljuk A, Niedermayer C, Ouladdiaf B, Hoser A, Hofmann T and Keimer B 2012 *Phys. Rev. B* **85** 184109
[41] Hsieh S H *et al* 2017 *Sci. Rep.* **7** 161
[42] Ishikawa T, Park S K, Katsufuji T, Arima T and Tokura Y 1998 *Phys. Rev. B* **58** R13326–9
[43] Zhu Y *et al* 2018 *Nat. Commun.* **9** 1799
[44] Fujioka J, Ishiwata S, Kaneko Y, Taguchi Y and Tokura Y 2012 *Phys. Rev. B* **85** 155141